Odor quality coding and categorization in human posterior piriform cortex

James D Howard, Jane Plailly, Marcus Grueschow,
John-Dylan Haynes, and Jay A Gottfried

Supplementary Figures

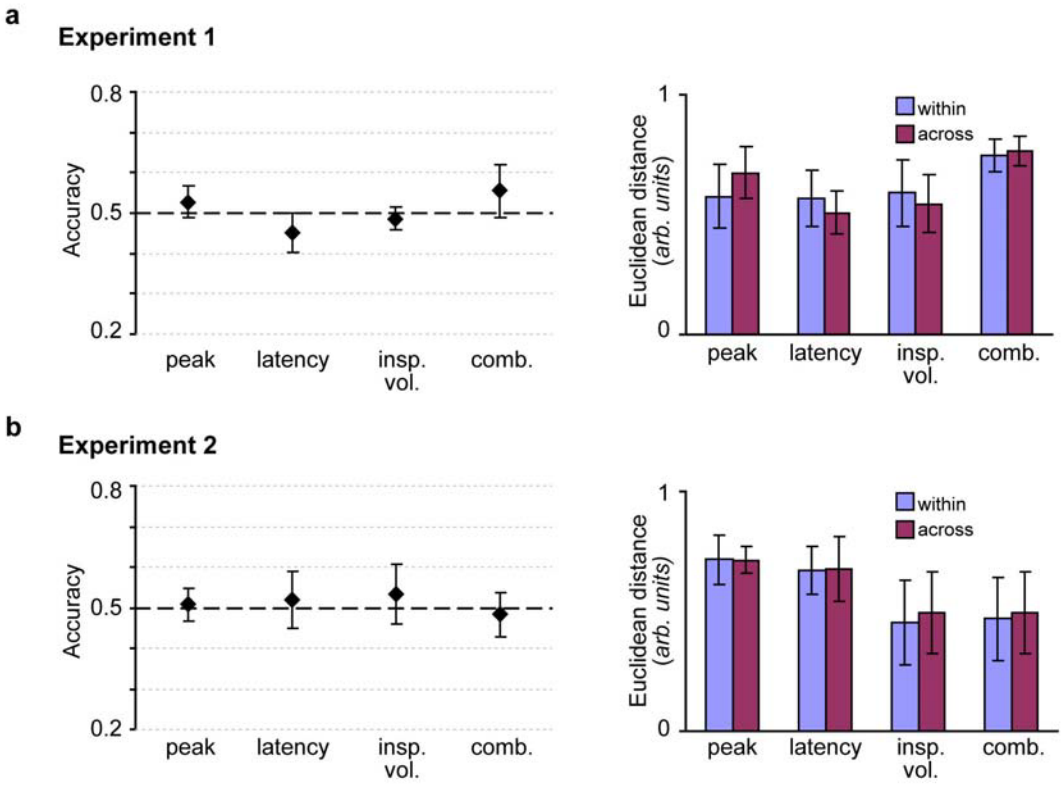

Supplementary Figure 1. Split-halves odor classification analysis using trial-specific sniff parameters. **(a)** Odor identification accuracy in Experiment 1 was not significantly different from chance for sniff peak ($T_5 = 0.70$, $P = 0.26$), duration ($T_5 = –1.02$, $P = 0.18$), inspiratory volume ($T_5 = -0.50$, $P = 0.32$), or a combination of these three parameters ($T_5 = 0.84$, $P = 0.22$). Furthermore, there were no significant differences between within- and across-odor distances for any of these parameters (P's = 0.24, 0.41, 0.38, and 0.82). **(b)** Odor category accuracy in Experiment 2 was not significantly different from chance for sniff peak ($T_3 = 0.19$, $P = 0.43$), duration ($T_3 = 0.28$, $P = 0.40$), inspiratory volume ($T_3 = 1.60$, $P = 0.10$), or the three-parameter combination ($T_3 = –0.30$, $P = 0.39$), nor were there significant differences between within- and across-category distances for any of the four parameters (P's = 0.99, 0.95, 0.13, and 0.36).

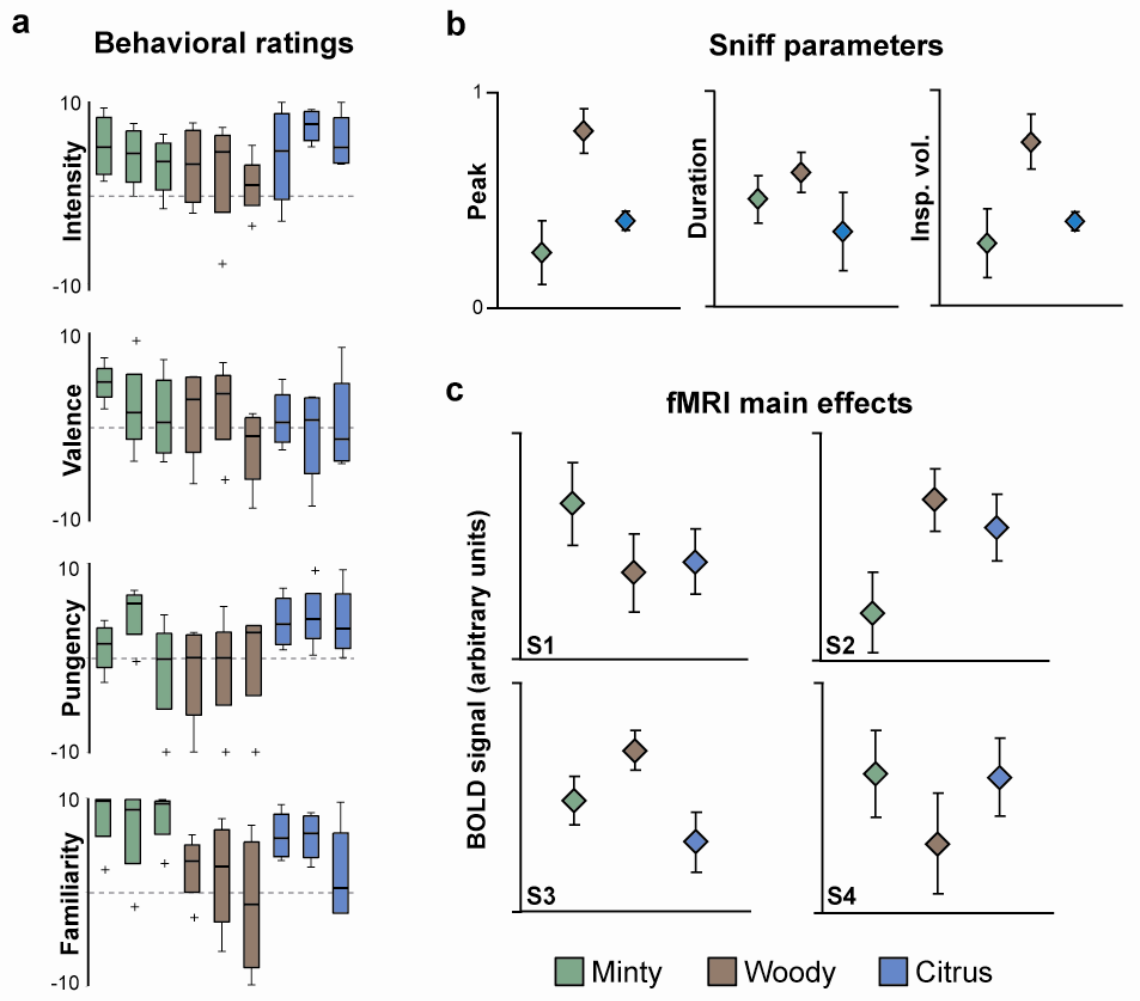

Supplementary Fig. 2. Behavioral ratings, sniff parameters, and fMRI main effects analysis for Experiment 2. **(a)** Boxplots show that group-averaged behavioral ratings did not significantly differ across the 9 odorants in odor intensity ($F_{8,27} = 0.84$, $P = 0.58$, one-way ANOVA), valence ($F_{8,27} = 0.67$, $P = 0.71$), pungency ($F_{8,27} = 1.24$, $P = 0.31$), or familiarity ($F_{8,27} = 1.72$, $P = 0.14$). **(b)** Mean normalized respiratory values (± between-subjects s.e.m.) are plotted for sniff peak, duration, and inspiratory volume (insp. vol.), none of which significantly differed between the three odor quality categories (peak, $F_{2,9} = 2.81$, $P = 0.19$; duration, $F_{2,9} = 0.72$, $P = 0.48$; insp. vol., $F_{2,9} = 4.96$, $P = 0.11$). **(c)** Category-specific mean blood oxygen level-dependent (BOLD) signal (± between-runs s.e.m.) in PPC is plotted for each subject. Signal on the *y*-axis is in arbitrary units. One-way ANOVAs testing for an effect of odor quality category on BOLD signal were not significant for 3/4 subjects (S1, $F_{2,69} = 0.96$, $P = 0.39$; S2, $F_{2,69} = 2.80$, $P = 0.067$; S4, $F_{2,69} = 0.79$, $P = 0.46$). Despite a significant effect in Subject 3 (S3, $F_{2,69} = 3.39$, $P = 0.040$), follow-up tests showed that not all categories could be discriminated from the others (Minty vs. Woody, $T_{46} = 1.60$, $P = 0.12$; Minty vs. Citrus, $T_{46} = 1.08$, $P = 0.28$).

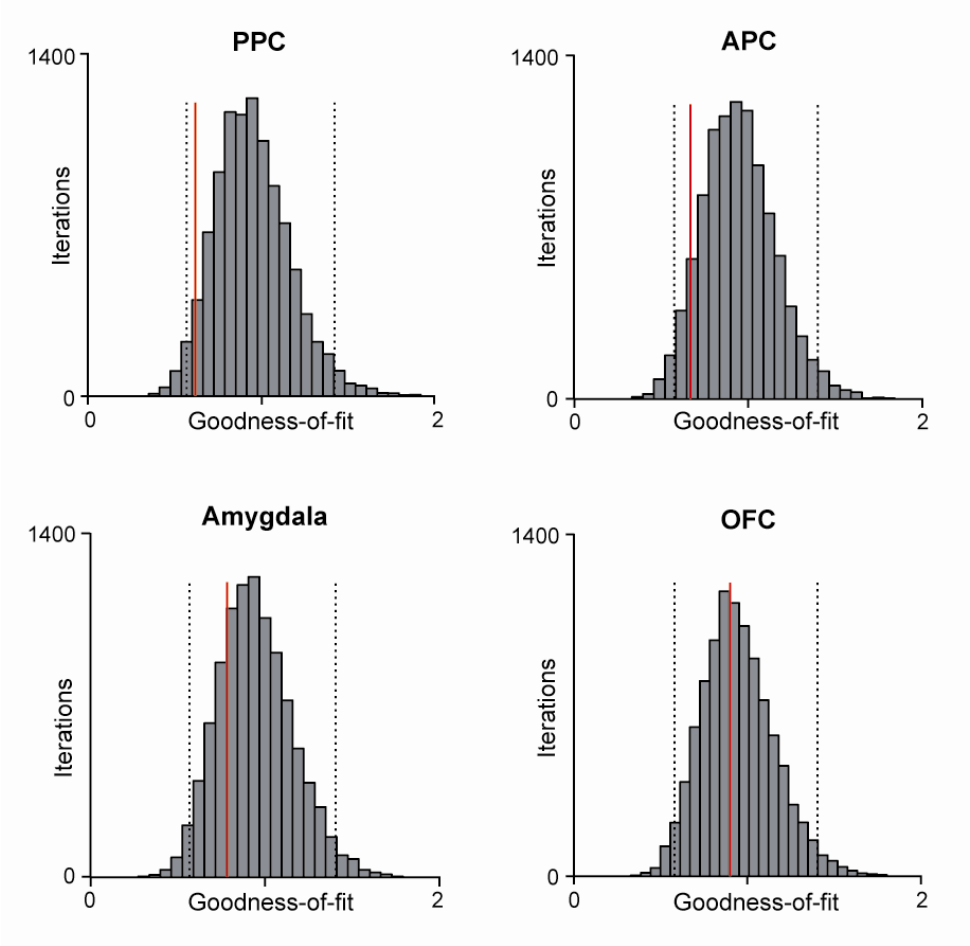

Supplementary Fig. 3. Alignment of odorant-specific fMRI spatial ensemble patterns (from Experiment 2) and odorant molecular features. The observed goodness-of-fit (solid red line) between three-dimensional MDS (multidimensional scaling) projections of imaging correlations (for each olfactory brain region) and odorant molecular features (based on Haddad et al., 2008)[12] is plotted against goodness-of-fit distributions randomly generated by a permutation analysis of the actual imaging data (10,000 iterations) (see **Main text**). The red lines fell within the 95% confidence interval (dashed lines) in each of the four regions, demonstrating that fMRI spatial patterns of activation do not significantly align with odorant molecular features.

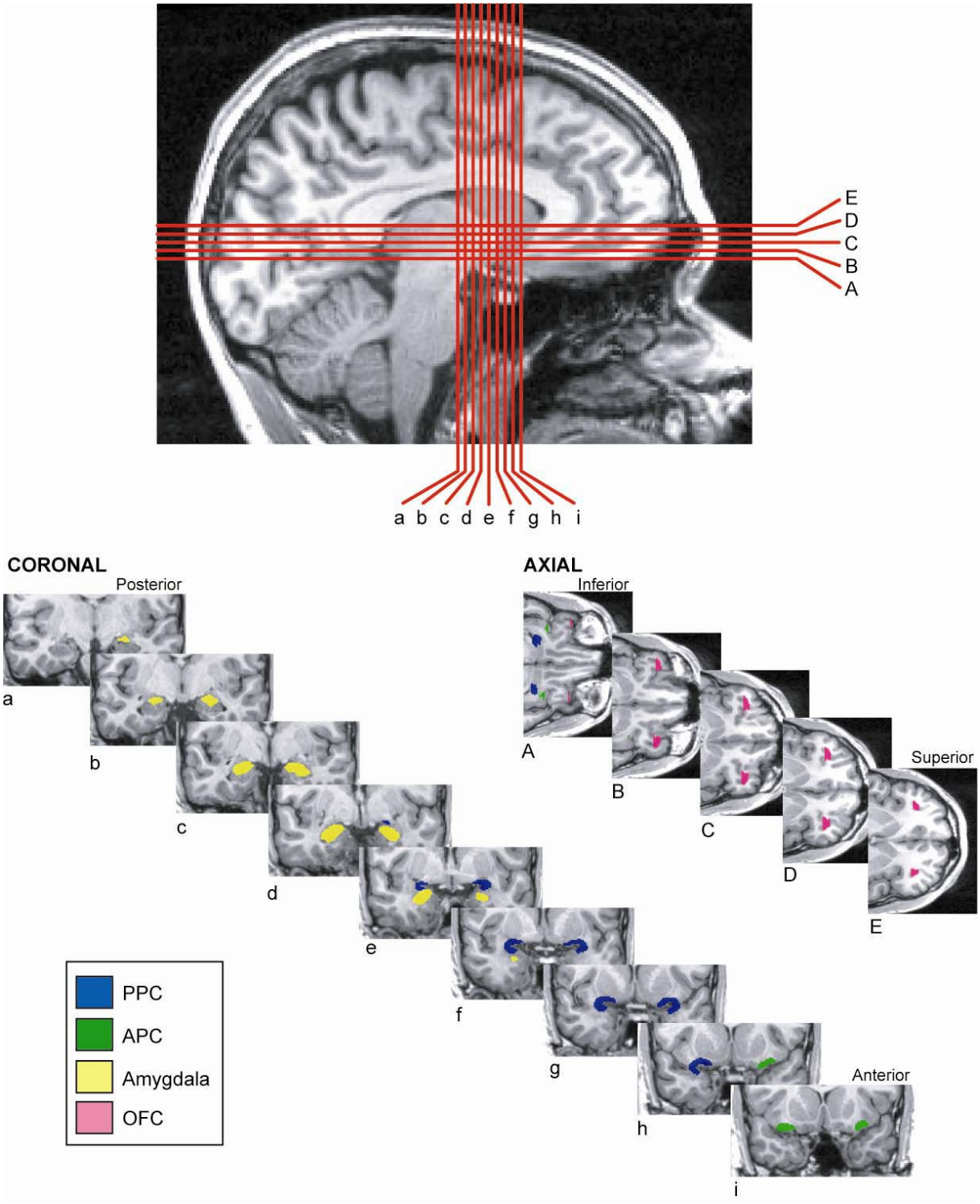

Supplementary Fig. 4. Olfactory regions of interest (ROIs), including posterior piriform cortex (PPC), anterior piriform cortex (APC), amygdala, and orbitofrontal cortex (OFC), are depicted on T1-weighted MRI scans from one subject. Spacing between each slice is 3 mm. The nine coronal slices (a-i) range from the posterior extent of amygdala to the anterior extent of APC. The five axial slices (A-E) span the extent of olfactory OFC.

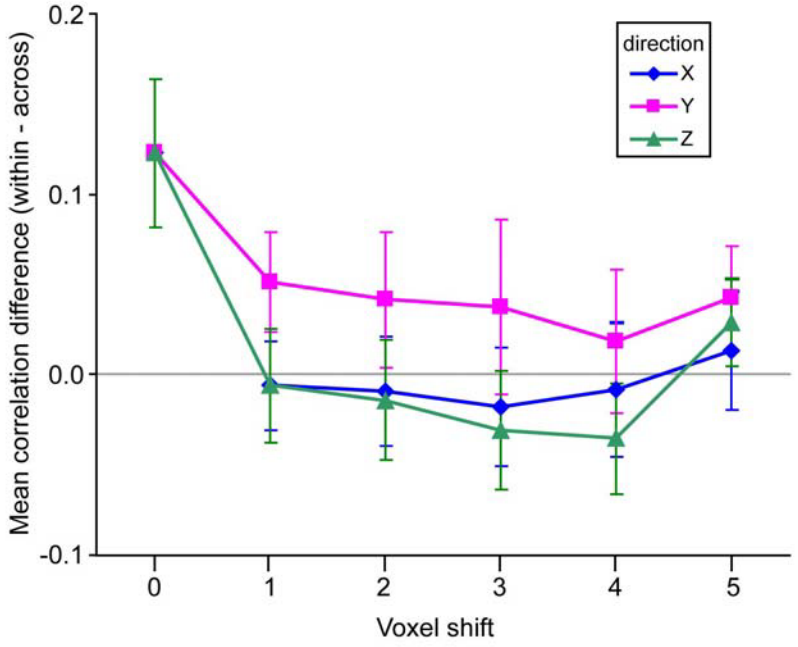

Supplementary Fig. 5. Across-days validation of spatial realignment. Within-odorant minus across-odorant correlation (mean ± between-subjects s.e.m.) as a function of incremental voxel shifts in posterior piriform cortex (odd vs. even runs). A one-voxel shift in the *x* or *y* direction amounted to a shift of 1.72 mm, while a one-voxel shift in the *z* direction amounted to a shift of 3.0 mm. The data show that the mean correlation difference was maximal at zero-voxel shift (reflecting the parameters actually utilized in the study) and progressively diminished with increasing voxel offset in the *x*, *y*, or *z* direction.

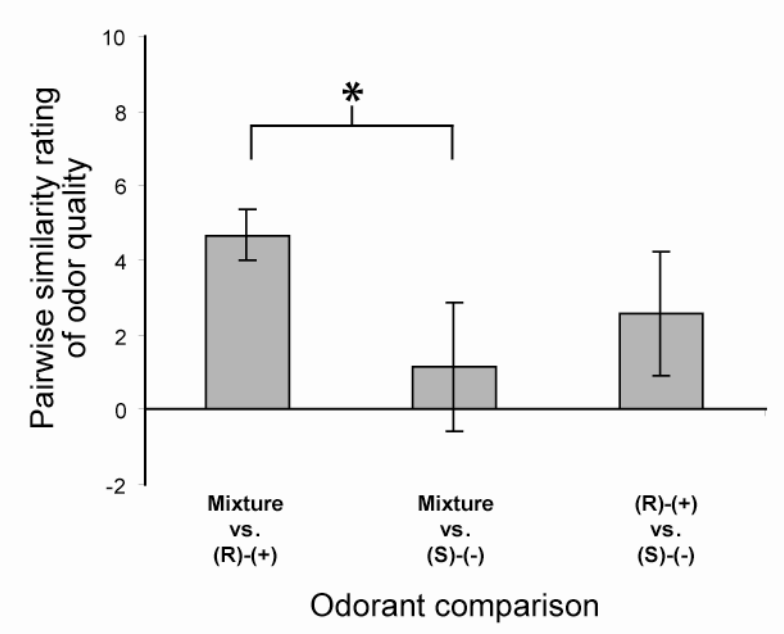

Supplementary Fig. 6. Pairwise similarity ratings of odor quality between the racemic citronellol mixture and its chiral components. Mean similarity rating (± between-subjects s.e.m.) are plotted for each pairwise rating. The similarity between the racemic mixture and the (R)-(+) enantiomer was significantly higher than the similarity between the mixture and the (S)-(-) enantiomer. No other comparison was significant. (*, $P < 0.05$, two-tailed paired *t*-test).

Supplementary Table 1

List of odorant descriptors included in each perceptual category for the behavioral analysis of odor quality in Experiment 2 (Figure 5c)

Perceptual category	Descriptor name	Dravnieks index no.*
Minty	herbal, green, cut grass	5
	camphor like	17
	cool, cooling	20
	eucalyptus	30
	minty, peppermint	40
	medicinal	59
Woody	musty, earthy, moldy	15
	woody, resinous	45
	bark-like, birch bark	65
	cedarwood-like	85
	rope-like	87
	cardboard-like	90
	cork-like	110
	oak wood, cognac-like	127
	hay	140
Citrus	sour, acid, vinegar	7
	cantaloupe, honeydew melon	28
	fruity (citrus)	42
	orange (fruit)	60
	lemon (fruit)	91
	pineapple (fruit)	113
	grapefruit	128
Floral	floral	52
	rose-like	66
	geranium leaves	82
	violets	106
	lavender	111
Berry	fruity (other)	43
	strawberry-like	108
	grape-juice like	129
	cherry (berry)	144
Spicy	cinnamon	25
	spicy	37
	anise (licorice)	56
	black pepper-like	78
	clove-like	138

*****Numbers refer to the descriptor index numbers found in the Dravnieks Odor Quality Evaluation [Dravnieks, A. *Atlas of odor character profiles* (ASTM, Philadelphia, 1985)].

Supplementary Data

Additional psychophysical characterization of the citronellol odorant

The citronellol odorant in Experiments 1 and 2 was selected for its "citrus-like" perceptual quality. The citronellol odorant used here was a racemic mixture of two optical isomers, only one of which is citrus-like: (R)-(+)-β-citronellol is described as having a citrus-like odor, whereas (S)-(–)-β-citronellol is described as having a geranium-like odor[1]. We have used the racemic mixture frequently in our prior studies (e.g., Gottfried et al., *Neuron* 2006, Figure 2)[2], and participants have consistently reported this to have a citrus character. In addition, as noted by Wise and colleagues (*Chem. Senses* 2000, Figure 4)[3], cluster analysis of Zwaardemaker's original odor classification scheme places citronellol within the group of citrus odors.

Nevertheless, to confirm that the citronellol racemic mixture is perceived as a citrus-like odor, we asked 10 additional participants to provide pairwise similarity ratings of odor quality between the racemic mixture and each of the pure isomers. As shown in **Supplementary Fig. 6** the similarity between the mixture and the (R)-(+) odorant was greater than the similarity between the mixture and the (S)-(–) odorant ($T_9 = 2.55$, $P = 0.031$; two-tailed paired t-test). No other pairwise test was significant, indicating that the quality of the racemic mixture most closely resembles the quality of the (R)-(+) isomer, that is, the citrus-like isomer.

Effects of odor pleasantness and intensity on PPC pattern correlation

To assess whether the observed imaging correlation differences (cf. **Fig. 3b**,**d**) partially reflected information about other perceptual features, we conducted two complementary analyses. Based on each subject's own ratings, the four odorants were arranged into a "more pleasant" group containing the two stimuli with higher valence ratings, and a "more unpleasant" group containing the two stimuli with lower valence ratings. The corresponding linear vectors were divided into even and odd runs, enabling us to compare within-valence correlations (e.g., pleasant/even runs vs. pleasant/odd runs) to across-valence correlations (e.g., pleasant/even runs vs. unpleasant/odd runs) in PPC. Similar procedures were used to evaluate odor intensity (using "more intense" and "less intense" groups of two odorants each). There was no significant mean correlation difference in either valence ($T_5 = 1.94$, $P = 0.11$) or intensity ($T_5 = 0.72$, $P = 0.51$), suggesting that neither of these perceptual characteristics alone contributed to odor-specific pattern differences in fMRI activity.

Note that behavioral ratings of odorant intensity, valence, pungency, and familiarity were not collected on a trial-by-trial basis. As such, we were not able to incorporate these measures into a split-halves classification analysis to assess them for odor-specific content (as was done with mean fMRI activity and sniff parameter data). However, the fact that the mean fMRI activity level in amygdala was not associated with significant odor classification performance in either experiment (cf. **Fig. 3c**,**e** and **Fig. 6c**,**d**), suggests that arousal, and perceived intensity for that matter (which is known to elicit responses in amygdala[4,5]), are unlikely to account for odor-specific pattern differences in PPC. Similar null findings with OFC mean activity levels suggest that perceived valence

(which is known to elicit responses in OFC[4,6]) would also not easily explain the pattern differences in PPC.

Validation of spatial alignment

In conventional fMRI analyses, image pre-processing includes spatial realignment, normalization to a standard template image, and smoothing (typically 8-10 mm). Although such procedures will obscure information that might be contained at the level of single voxels and individual subjects, they have the advantage of simplifying statistical analysis and enabling population-based hypothesis testing[7]. An additional benefit is that one does not need to assume that voxels are in precise spatial register from the beginning to the end of a scanning session, or from one day to the next, since spatial pre-processing tends to blend information across neighboring voxels.

In the fMRI analyses described here, images from the three days of scanning were spatially realigned using SPM2 software, but normalization and smoothing were not performed, in order to maximize signal fidelity within individual voxels and to characterize spatial patterns of fMRI activity across voxel ensembles. However, these multivariate fMRI approaches implicitly rely on the assumption that voxel *n* on the "even" runs is identical to voxel *n* on the "odd" runs, or more generally, that voxels are precisely realigned across each of the three scanning days.

Although any computational shortcomings of spatial realignment would only weaken the effects described here, we set out to validate image realignment by testing the effect of spatial *mis*-alignment on PPC correlations. The correlations between realigned "even" and "odd" runs (within-odor vs. across-odor, Experiment 1) were computed after incremental voxel shifts in the "even" data set, in each of the three imaging axes: *x*, *y,* and *z* (**Supplementary Fig. 5**). Correlations were averaged across offsets in the "plus" and "minus" directions (e.g., +2 and -2), to yield correlation values for each absolute shift in any voxel dimension. The prediction was that if our observed results were simply due to methodological artifact, then systematic spatial misalignment should have no effect on the linear correlations. On the other hand, if our findings reflected accurate voxel alignment across scans and days, then increasing spatial misalignment of the images should cause progressive decline in the correlations.

Plots of correlation values against voxel offsets (**Supplementary Fig. 5**) confirmed the latter prediction: correlations were maximal at the un-shifted point in each direction (*x*, *y,* and $z = 0$), whereas these correlations were reduced by as little as a one-voxel shift in any of the three directions. Pairwise *t*-tests demonstrated that the difference between within- and across-odor correlations in the zero-voxel-shift condition was significantly greater than the correlation difference in the 1-voxel-shift condition in both the *x* and *z* directions ($T_5 = 2.92$, $P = 0.033$; $T_5 = 3.05$, $P = 0.028$, respectively), and was significantly greater than the correlation difference in the 4-voxel-shift condition in the *y*-direction ($T_5 = 2.146$, $P = 0.042$). These findings demonstrate that the correlations across voxel ensembles of PPC activity are highly sensitive to minor offsets in realignment, and indicate that our realignment procedure was optimal for computing pattern-based linear fMRI correlations.

As an additional measure of realignment fidelity, we computed the mean realigned functional image for each of the three days separately, and then realigned these day-averaged mean images to each other, on a subject-by-subject basis. The resulting parameters from this realignment, representing the degree of shift required to align the three mean images, were all less than 10^{-11} mm for each subject, further suggesting that spatial realignment was sufficiently reliable and robust to permit inference testing at the level of individual voxels across days.

Supplementary Discussion

To the extent that the fMRI (BOLD) signal is an indirect measure of population field potentials and local input processing, as opposed to signal outputs and spike firing[8], it is certainly possible that the PPC patterns observed here are an echo of afferent input arising from upstream areas. Interestingly, single-unit studies by Schoenbaum and colleagues, and Wilson and colleagues, seem to suggest that basic sensory information about an odor is encoded in anterior piriform neurons[9,10], whereas odor "meaning" is encoded in posterior piriform neurons[9,11], perhaps on the basis of stronger amygdala input and other associative links. Therefore, given these observations, our fMRI data showing olfactory categorical perception in PPC would be in keeping with their conclusions that posterior piriform is more responsive to the meaning of an odor. We would also add that the absence of significant ensemble activity in either APC or amygdala further complements the idea that the activity patterns in PPC likely reflect encoding of information about odor quality.

Supplementary References

1. Laska, M. & Teubner, P. Olfactory discrimination ability of human subjects for ten pairs of enantiomers. *Chem. Senses* **24**, 161-170 (1999).

2. Gottfried, J.A., Winston, J.S. & Dolan, R.J. Dissociable codes of odor quality and odorant structure in human piriform cortex. *Neuron* **49**, 467-479 (2006).

3. Wise, P.M., Olsson, M.J. & Cain, W.S. Quantification of odor quality. *Chem. Senses* **25**, 429-443 (2000).

4. Anderson, A.K.*, et al.* Dissociated neural representations of intensity and valence in human olfaction. *Nat. Neurosci.* **6**, 196-202 (2003).

5. Winston, J.S., Gottfried, J.A., Kilner, J.M. & Dolan, R.J. Integrated neural representations of odor intensity and affective valence in human amygdala. *J. Neurosci.* **25**, 8903-8907 (2005).

6. Gottfried, J.A., Deichmann, R., Winston, J.S. & Dolan, R.J. Functional heterogeneity in human olfactory cortex: an event-related functional magnetic resonance imaging study. *J. Neurosci.* **22**, 10819-10828 (2002).

7. Kriegeskorte, N. & Bandettini, P. Analyzing for information, not activation, to exploit high-resolution fMRI. *Neuroimage* **38**, 649-662 (2007).

8. Logothetis, N.K., Pauls, J., Augath, M., Trinath, T. & Oeltermann, A. Neurophysiological investigation of the basis of the fMRI signal. *Nature* **412**, 150-157 (2001).

9. Kadohisa, M. & Wilson, D.A. Separate encoding of identity and similarity of complex familiar odors in piriform cortex. *Proc. Natl. Acad. Sci. U.S.A.* **103**, 15206-15211 (2006).

10. Roesch, M.R., Stalnaker, T.A. & Schoenbaum, G. Associative encoding in anterior piriform cortex versus orbitofrontal cortex during odor discrimination and reversal learning. *Cereb. Cortex* **17**, 643-652 (2007).

11. Calu, D.J., Roesch, M.R., Stalnaker, T.A. & Schoenbaum, G. Associative encoding in posterior piriform cortex during odor discrimination and reversal learning. *Cereb. Cortex* **17**, 1342-1349 (2007).

12. Haddad, R.*, et al.* A metric for odorant comparison. *Nat. Methods* (2008).